Material characterization of a 3D-woven carbon fiber preform at macro-scale level for manufacturing process modeling

George Scarlat[1], Raj Ramgulam[1], Per Martinsson[2], Kent Kasper[1], Harun Bayraktar[1]

[1]Albany Engineered Composites Inc., Rochester NH, USA
[2]Albany International AB, Halmstad, Sweden

1 Introduction

The present paper showcases the work done at Albany Engineered Composites (AEC) to characterize and model the mechanical behavior of the 3D woven carbon fiber preform at the macroscopic level with the purpose of numerically simulating the forming processes that take place within the manufacturing of advanced composite components for the aero industry. Some examples include the lift fan components for the F-35 Joint Strike Fighter, main landing gear brace for the Boeing 787 Dreamliner, and components for the CFM LEAP aero engines that power the Boeing 737-MAX and Airbus A320neo. These composites are manufactured using preforms that are 3D woven and undergo a complex forming process during manufacturing prior to being injected with resin during the RTM process.

A variety of factors during the forming process can have a significant effect on the quality of the preform as it arrives at the RTM injection stage. A “good” preform quality usually means the absence of any wrinkles, high-shear areas and other similar local flaws at the end of the forming process, minimizing any processing effects on the performance of the molded part.

The use of Finite Elements Analysis (FEA) tools can help predict such local defects, and allows the exploration of different combinations of system and process parameters. This would have the end result of both enhancing the quality of the components manufactured as well as helping reduce the cost associated with both design and manufacturing through a better understanding of the 3D-woven preform behavior during the process. Due to the availability of multiple material models that mimic dry-fabrics behavior, its speed, and robustness of its contact algorithm, LS-DYNA FEA software was chosen to model the forming processes for 3D-woven carbon fiber preforms.

This paper is organized as follows: Section 2 presents some general considerations in building the FEA models for the purpose of this work. Section 3 describes the experimental coupon tests undertaken for model calibration purpose and shows some representative results. Section 4 examines the details of the FE models used and presents some results assessing the fidelity of the numerical models as compared with respective experimental data collected. Finally, Section 5 summarizes the current work and presents some conclusions.

2 Considerations in building FEA models for 3D-woven preforms

2.1 Model scale

The FEA method has been used to model 3D-woven preforms at any of the following three levels, depending of the analysis purpose: macro-scale (the discrete tow architecture is modelled as a continuum), meso-scale (each individual tow is represented) and micro-scale (each filament in the tow is modeled individually).

Figure 1 shows a 4 x 4 unit cell of a typical ply-to-ply architecture of a 3D-woven preform at the meso-scale level. The tow paths in the various numbered section-cut planes through both the warp (blue) and weft (red) columns show the structural integrity of the ply-to-ply inter-lock architecture. 3D-woven composites have demonstrated advantages over the conventional laminated composites: absence of

the de-lamination mechanism during loading, superior energy absorption and increased impact damage tolerance [1].

Previously reported efforts at AEC dealt with modeling the preform at the meso-scale level [2] to create predictive FEA models that replicate the forming process of preforms for rather small-sized structures. Because the ultimate goal of the present effort was to numerically simulate forming of large-size components, a macro-scale approach was required.

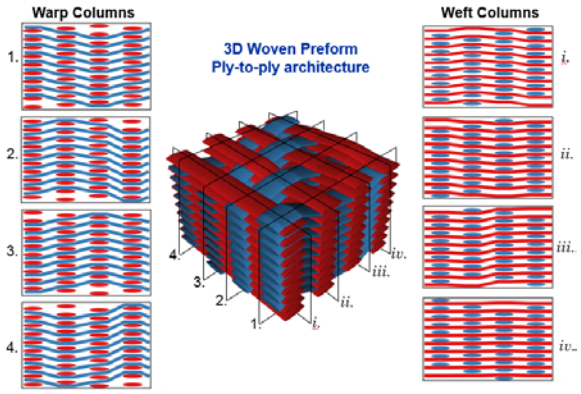

Fig.1: 3D-woven preform unit cell (4 x 4) at mesoscale level

At AEC, efforts will continue towards developing and methodically validating our meso-scale modelling capabilities, such that meso-scale FE models of 3D-woven preform will be used as virtual testing platforms, replacing the physical testing, to generate constitutive data for the macro-scale FE models. These, in turn, that will be used to numerically simulate certain manufacturing processes.

2.2 Material model

From a numerical material model point of view, the choice was either to develop a user-defined material model, or to test some of the already built-in material models in the LS-DYNA material library. It was decided to take the latter approach, and based on a review of the available fabric models as well as communication with LSTC technical support, the following were judged as potential good candidates [3]: MAT_034 (MAT_FABRIC), MAT_214 (MAT_DRY_FABRIC), MAT_234 (VISCOELASTIC_LOOSE_FABRIC), MAT_235 (MICROMECHANICS_DRY_FABRIC) and MAT_249 (REINFORCED_THERMOPLASTIC). MAT_234 and MAT_235 proved unsuitable for the end goal since their initial fiber orientation is always at a 45 degree angle with the shell edges, and for the forming process FEA we need to have the fiber aligned with the shell edges, which themselves must follow the component contours. MAT_249 presented a different challenge as a relatively recent addition to the material library, whose calibration process was repeated several times as new info became available.

All these material models require using shell elements for modeling the 3D-woven preform. It is understood that the use of shell elements would remove the possibility of modeling any through-thickness behavior of the 3D-woven preform during forming, and this was noted as a first limitation at this stage. Depending on the fidelity in matching physical tests, this might be revisited later.

2.3 Loading

Based on observations from the physical forming process, it was determined that the main loading mechanisms acting on the preform are in-plane, essentially tensile and shear. These mechanisms can be potentially taken into account by calibrating the behavior of the numerical material model based on the fidelity in matching representative experimentally measured response of the 3D woven preform material coupons.

3 Experimental tests

Four types of preform architectures were tested at the coupon level to assess the effect of tow size on the in-plane and out-of-plane response (Table 1). The warp tow's size is being progressively increased from one type to the other e.g. considering type-A preform warp tow size is N – where N is a multiple of 1000 filaments – then type-B preform is 2N, type-C is 3N and type-D is 4N.

	Type-A	Type-B	Type-C	Type-D
Fiber topology	Same for all			
Fiber type	Intermediate modulus carbon fiber			
No of layers	Same for all			
No of filaments (warp)	N	2N	3N	4N
No of filaments (weft)	Same for all			
Thickness [mm]	5	6	7	8

Table 1: 3D-woven architectures types tested

Following a similar methodology described in earlier studies [4], several types of experimental tests at coupon level were performed with the goal of helping characterize the preform in-plane behavior (e.g. uni-directional tensile, picture-frame and bias-extension). They represent the focus of present paper.

3.1 Uni-directional Tensile tests

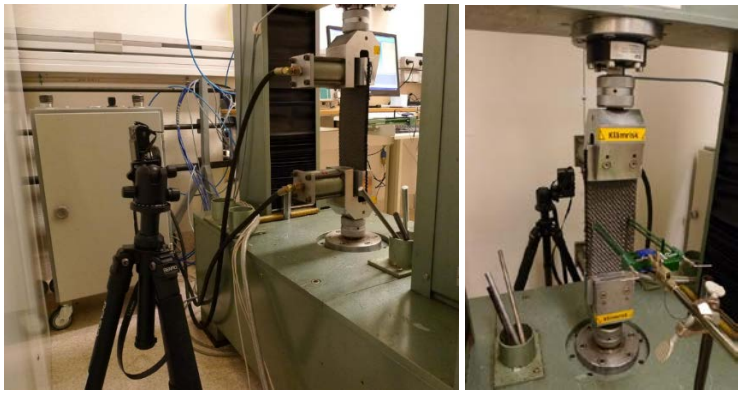

Fig.2: Experimental setup used for the tensile tests

The preform coupon tensile tests were performed at the Albany International R&D test facilities in Halmstad, Sweden. Figure 2 shows a representative experimental setup that was used for the uni-directional tensile tests. The preform coupon is held using hydraulic clamps in a tensile tester machine, and a mechanical extensometer is used for measuring the lateral contraction of the preform, needed in determining the apparent Poisson's ratio.

The overall in-plane dimensions for all 3D-woven carbon preform coupons used in the tensile tests were 210 mm x 100 mm (L x W). The thickness of the samples are as per Table 1 above.

A computer-controlled data acquisition system automatically collected Force vs Displacement data during these tests and such data was post-processed further in order to create Stress vs Strain curves as shown in Figure 3 (here, stress is normalized to the highest value from type-A sample results).

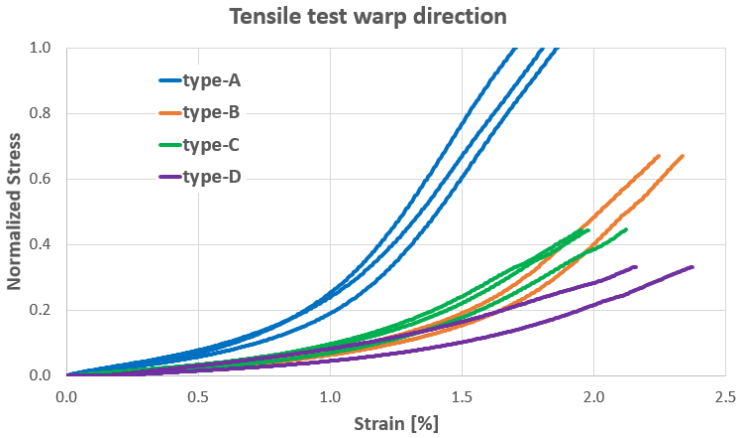

Fig.3: Representative results from the cyclic tensile loading tests

3.2 Picture-frame tests

The preform coupon picture-frame tests were performed at the Albany International test facilities in Bury, UK. Figure 4 shows the experimental setup used for these tests. The preform coupon was cut in a cruciform shape and was mechanically clamped in a specially-designed trellis frame constructed for this purpose. The trellis frame was mounted in a tensile tester such that the load applied would make an angle of 45 degrees with the preform tows.

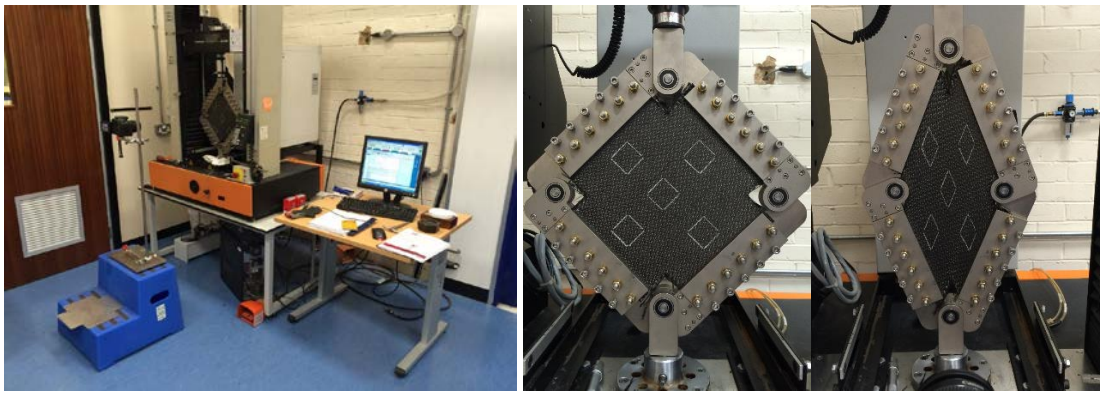

Fig.4: Experimental setup used for the picture-frame tests. Left: overview, middle: un-deformed specimen, right: deformed specimen

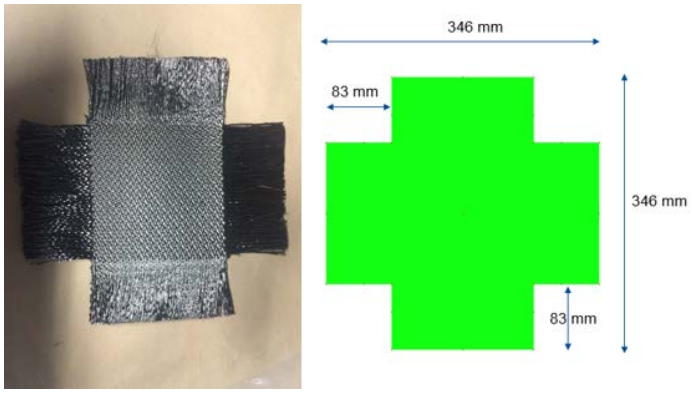

Fig.5: Cruciform-shape specimen for the picture-frame test

Figure 5 shows a cruciform-shape specimen (this one having un-raveled flanges) and its overall in-plane dimensions. Specimen thicknesses are as reported in Table 1.

A computer-controlled data acquisition system automatically collected the pulling force vs top-hinge vertical displacement data during these tests and such data was post-processed further in order to create Shear Force vs Shear Angle curves. A schematic of this post-processing calculation is shown in Figure 6, and representative results ranges for all specimen types are shown in Figure 7. Here, the shear force is normalized to the highest value from type-D sample results. Significant stiffening in the response can be noticed in the latter part of the response when yarn compaction, instead of shear, becomes the dominant mechanism.

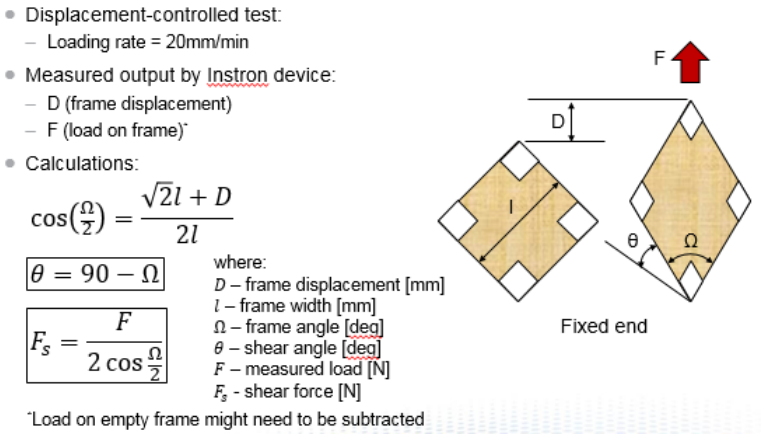

Fig.6: Shear Force vs Shear Angle calculation in the picture-frame test

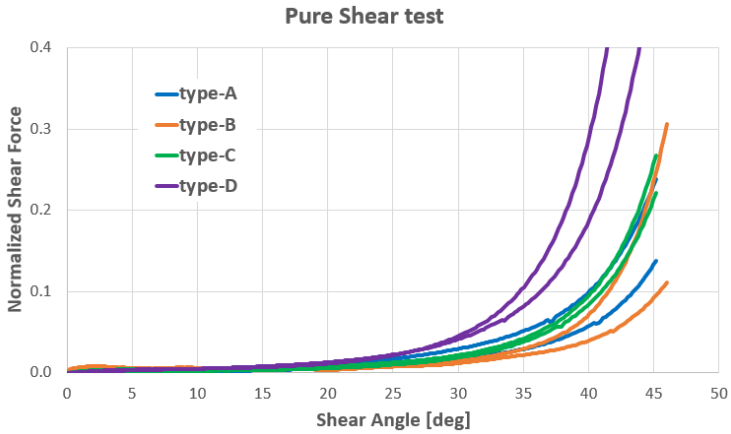

Fig.7: Representative response from the picture-frame test (ranges for specimens type-A and D)

3.3 Bias-Extension tests

The bias-extension test is extensively used to characterize shear in textile materials in general, due to its simplicity. However, it has some clear limitations, one of which being that only the central region of the specimen is in a pure state of shear. Thus, in the present study, it was only used as a supplementary validation tool, once the numerical material models' tensile and shear behaviour were already calibrated.

The preform coupon bias-extension tests were performed at the Albany International R&D test facilities in Halmstad, Sweden. The test setup, shown in Figure 8, is similar with the tensile test described above, except that the rectangular preform specimens were cut such that the fibers make a 45 degree angle with the loading direction. The white pins' square pattern can be noticed in the un-deformed state in the central region of the preform – where a state of pure shear is expected. This square pattern morphs into a rhombus one during testing, the acute angle of which is the complementary of twice the shear angle within the central region of the preform.

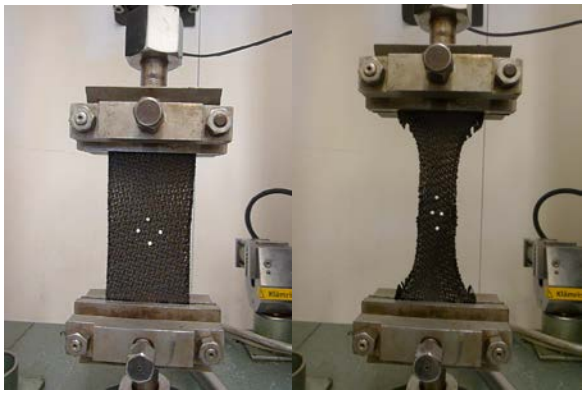

Fig.8: Un-deformed (left) and deformed (right) preform coupon used in bias-extension testing

4 Numerical simulations

Quasi-static FEA using the explicit solver were carried-out for all load cases and all materials. Besides ensuring level-playing field to enable response comparison of all material models (MAT_249 cannot be used with the implicit solver yet), this was done because the final goal was to numerically simulate the entire component forming process, for which a static analysis would not be useful.

Fully-integrated shell elements ELFORM=16 with hourglass control type IHQ=8 were used for all analyses. Material formulation FORM=24 was used for MAT_034.

All FE models shared the same model setup for each load case, respectively, and consistent material models (having both tensile and shear behaviour defined) were used for all of them. For the tensile tests, the a-axis fiber (i.e. warp) was aligned with the loading direction, the b-axis (i.e. weft) being orthogonal initially (see Figure 1 for warp and weft directions). For the picture-frame and the bias-extension tests the “a” and “b” fiber axes are orthogonal and at 45 degrees each with the loading direction, initially. This was achieved using the BETA parameter for MAT_214 and MAT_249, while in the case of MAT_034 the ICOMP=1 option in the SECTION_SHELL card was used in order to specify offset angles from the baseline a-axis direction as determined by the material axis option AOPT.

The constitutive material tensile response (in the form of stress vs uniaxial strain) for both MAT_034 and MAT_249 were obtained from representative force-displacement curves for each warp tow size coupon (i.e. type-A, B, C or D), recognizing that the load is carried only by the carbon fiber reinforcement (i.e. stress is computed considering only the carbon-fiber cross sectional area). In the case of MAT_214, its constitutive tensile response was calibrated by tuning the elasticity moduli for both the crimp and post-crimp regions of the piece-wise linear loading response to match the experimental coupon response.

Since MAT_249 was intended to replicate the behaviour of a woven fabric (i.e. only the reinforcement part of the response was desired) its matrix properties were set to small values so not to cloud the overall response.

The constitutive material shear response was input either as shear stress vs shear angle for MAT_249 or as 2nd Piola-Kirchhoff shear stress vs Green strain for MAT_034. The shear stress was obtained from the shear force acting only on the coupon’s carbon fiber area (taking advantage of the known fiber volume fraction of this particular architecture). For MAT_214, the shear moduli representing the slope of each of the three segment piecewise linear constitutive shear response were calibrated to fit the experimental coupon shear response.

4.1 Tensile coupon-test FEA

A simple FE model representative of the experimental coupon tensile test was constructed, with one end of the virtual specimen fixed and a prescribed motion applied at the other end, in a displacement-

controlled loading that matched the tensile tester's cross-head displacement recorded from experiments.

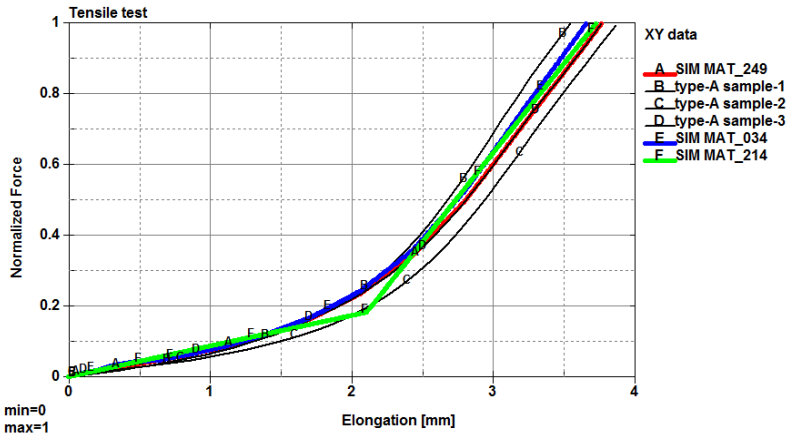

Fig.9: FE model for uniaxial tensile test and comparison with experimental data

Figure 9 shows a comparison of the normalized force vs elongation response between the FE model and the tensile test data from type-A coupons, using each of the three material models considered. As expected, Figure 9 shows overall good fidelity for each of the three material models matching physical coupon responses.

4.2 Picture-frame coupon-test FEA

For the picture-frame test, a FE model representative of the physical test was constructed as shown in Figure 10. The virtual preform coupon, with a cruciform shape, shares nodes with four rigid-body plates, which are connected two-by-two through rigid trusses by a total of four revolute joints. One end of the frame was fixed while the other end was pulled, in a displacement-controlled loading matching that of the tensile tester's cross-head recorded from experiments.

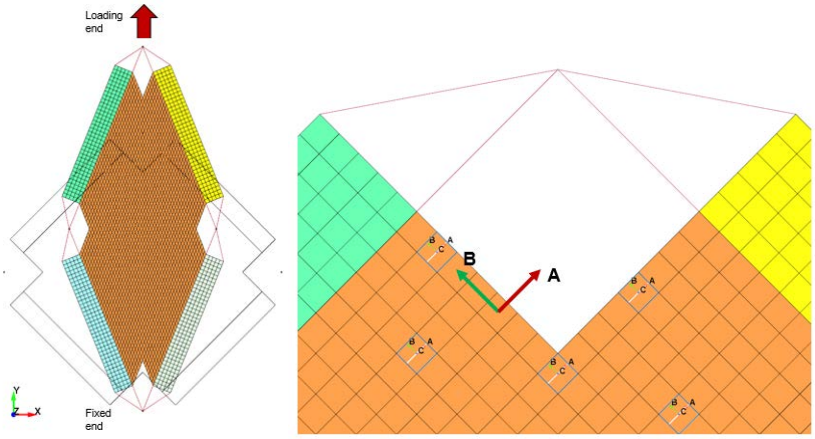

Fig.10: FE model of the picture-frame test: deformed shape with un-deformed outline (left); material orientation detail (right)

For MAT_249, METHxy=2 was used to model the elastic shear response. The authors are aware that, as of latter LS-DYNA version R9.0 [3], the recommended method for modelling elastic shear response in woven fabrics is METHxy=10, but this was not documented at the time of this work. Further tests will be performed to assess whether the recommended method is better suited for the particular 3D-woven preform analysed.

Figure 11 shows the normalized pulling force vs top-hinge displacement response from the FEA, in comparison with actual test data from type-D coupons. It also depicts a representative shear angle

fringe plot (in degrees, corresponding to MAT_249) showing good uniformity and levels similar to ones observed in the physical coupon tests.

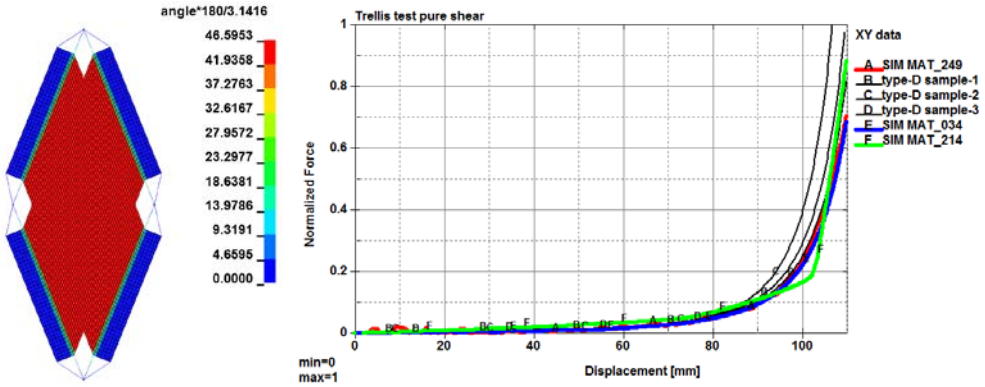

Fig.11: Picture-frame test: FEA vs experimental response (type-D specimen)

It can be noticed that both MAT_034 and MAT_249 show a very good correlation with experimental data. The response of MAT_214 shows again, as in the tensile test case, the lowest fidelity in replicating test data (not surprisingly, given the piecewise linear nature of its response).

Figure 12 shows comparison of normalized force vs displacement between MAT_249 model response and the experimental tests for each type of preform material (i.e. type-A, B, C and D). The good correlation seen in each of these cases – together with the similarly good correlation showed in the tensile tests case – indicates that MAT_249 is a valid choice for modelling the in-plane response of this 3D-woven preform.

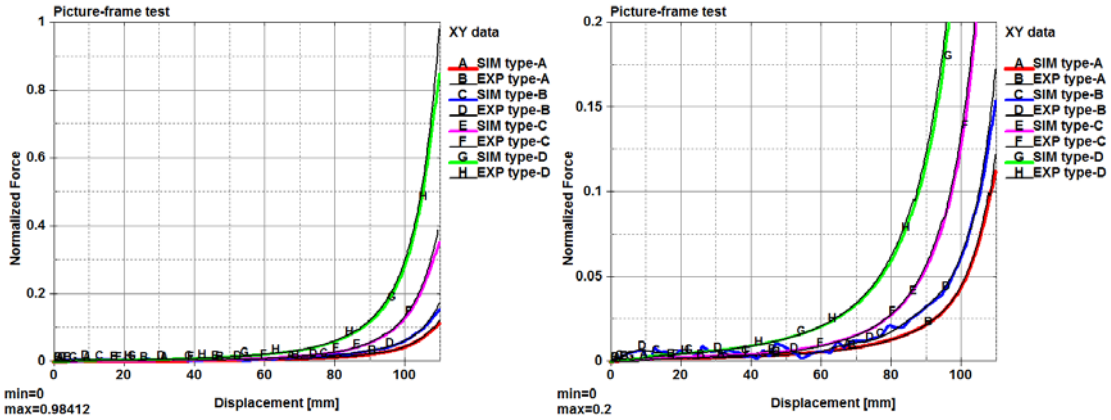

Fig.12: Picture-frame test: MAT_249 FEA vs experimental response for each tow size (detail, on right)

4.3 Bias-extension coupon-test FEA

After calibrating separately the tensile and shear responses of the material models analysed, the bias-extension test was used as a validation benchmark for the combined effects of these. Figure 13 shows the corresponding FE model built to replicate this type of test, in a representative elongated configuration. Similarly with the picture-frame test, the material model axes are initially orthogonal and arranged such that they each make a 45 degree with the loading axis. The shear angle between the fibers that is shown in the contour plot is representative for such type of loading, with a central rhomboidal region of pure shear, two end regions without shear and the rest of specimen showing a shear angle that is roughly half the max shear angle within the central region.

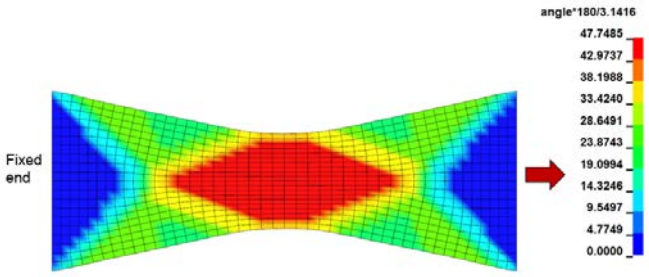

Fig.13: Bias-extension FE model showing shear angle contours for type-D preform (MAT_249)

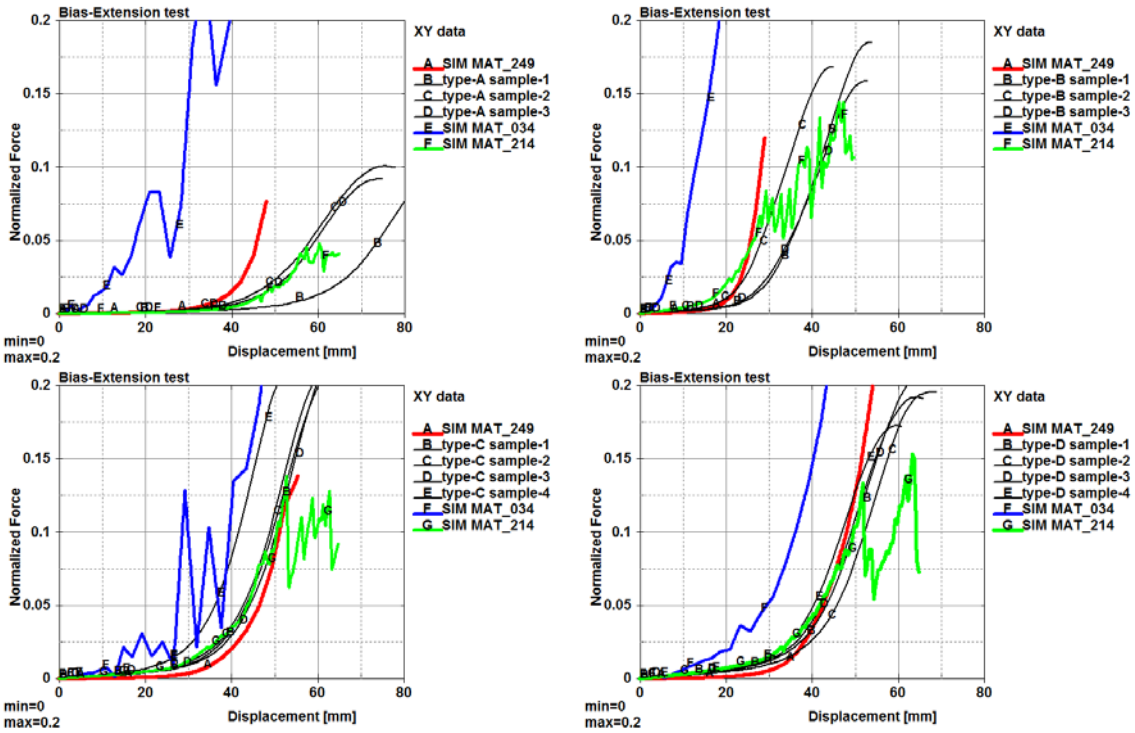

Fig.14: Bias-extension test: MAT_034 vs MAT_249 vs experimental response (all tow sizes)

Figure 14 shows the normalized force vs displacement comparison response for each of the MAT_034, MAT_214 and MAT_249 against experimental data, for all specimen types. Based on this comparison, the following conclusions can be drawn:

- MAT_034 is not able to represent the bias-extension response of this particular type of 3D-woven preform, for any specimen size, despite having both its tensile and shear behaviour validated separately against corresponding test data. It may be possible that the intrinsic tensile-shear coupling is not suitable to represent the kind of 3D-woven preform analysed.
- MAT_214 shows relatively good correlation for all specimen sizes, except at higher elongations. Its response, however, is noisier than MAT_249's, indicating a potential instability.
- The response of MAT_249 indicates good correlation for samples type-C and D. They are the thickest samples, with large warp tows size. The response of the thinnest samples (type-A and B) at large elongations is stiffer than the experimental data.
- In comparing the numerical and experimental force-displacement response of a bias-extension test, the inter-tow slip mechanism need to be considered [5], depending on the architecture of the preform analysed. This inter-tow slip mechanism might partially explain the stiffer FE model response observed, especially for the smaller tow size samples.

4.4 Draping FEA test

As a means to assess the draping behaviour of the three material models under consideration, a FE model was constructed representing a strip of type-D preform being pulled, along the warp direction, over a contoured mandrel. Figure 15 shows the un-deformed FE model, together with the final deformed shape for the three material models considered (MAT_034, MAT_214 and MAT_249). The good draping behaviour of MAT_249 even when tensioned over an exaggeratedly contoured part, as opposed to the other two, can be qualitatively established by the absence of numerical instabilities (e.g. wrinkles) which can be noticed in the other two cases. This is more in line with how a 3D-woven preform of this type would behave physically.

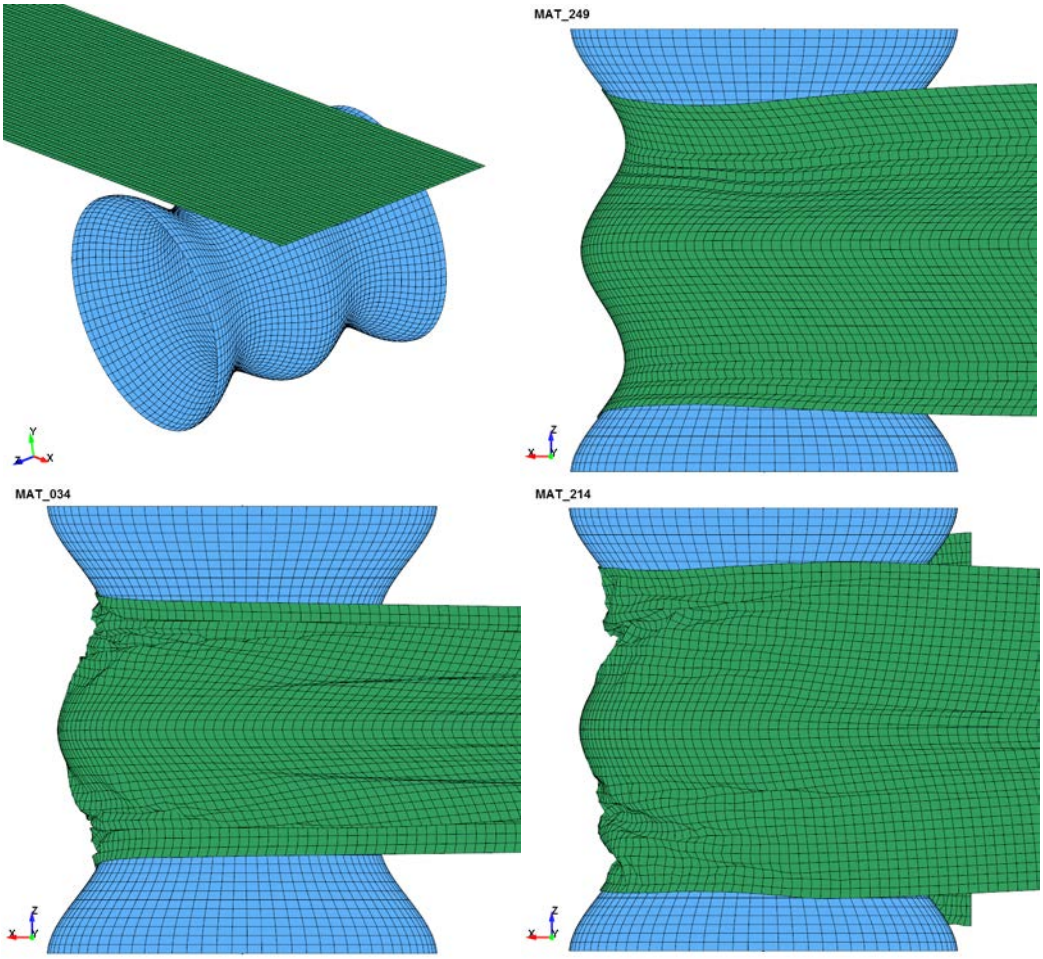

Fig.15: Draping FEA behaviour: un-deformed (upper left), MAT_249 (upper right), MAT_034 (lower left) and MAT_214 (lower right)

5 Summary and Conclusions

The current paper presents the results of an initial study meant to evaluate the potential use of some off-the-shelf material models available in LS-DYNA to replicate at a macro-scale level the 3D-woven carbon preform behaviour used for manufacturing composite components of the latest generation aero engines and structures. The final goal of this effort is to numerically simulate the entire forming process of such components.

Several built-in material models in LS-DYNA were evaluated for this purpose. The results of three of them (MAT_034, MAT_214 and MAT_249) were shown for the following load cases: uni-axial tension, shear, bias-extension and draping.

While MAT_034 showed, independently, good tensile and shear behaviour fidelity vs corresponding experimental data, its combined tensile and shear response was a poor match for the coupon response in the bias-extension test. Likewise, its draping behaviour was a poor match compared with the behaviour of physical samples of this type of 3D-woven preform.

MAT_214 did not show as good of a correlation with test data from the tensile and shear tests as MAT_034 and MAT_249. It showed a relatively good (albeit noisy) response correlation with test data in the bias-extension test. Its draping behaviour was unrealistic, as in MAT_034 case. As opposed to the other two material models analysed, the need to calibrate MAT_214 piecewise linear constitutive response made it unsuitable for embedding in predictive numerical simulation workflows.

The results obtained using MAT_249 material model achieved generally good fidelity in matching the in-plane response of the 3D-woven preform. Likewise, it showed good draping behaviour. As such, this material model was deemed to best represent at a macro-scale level the response of this kind of 3D-woven carbon fiber preform. It will be used in subsequent forming FEA simulations to be carried on in future work.

6 Literature

[1] Goering, J., Bayraktar, H.: “3D Woven Composites for Energy Absorption Applications”, SAE Technical Paper 2016-01-0530, 2016

[2] Bayraktar, H., Ehrlich, D., and all: “Forming and performance analysis of a 3D-woven composite curved beam through meso-scale FEA”, SAMPE Journal 51, p. 23-29, 2015

[3] LS-DYNA Keyword User’s Manual, Volume II, LS-DYNA R9.0, Lawrence Livermore Software Technology Corp (LSTC), 2016

[4] Cao, J., Akkerman, R., Boisse, P., Chen, J., Harrison, P., Lomov, S.V., Tao, X. M., and all: “Characterization of mechanical behavior of woven fabrics: Experimental methods and benchmark results”, Journal of Composites part A: Applied Science and Manufacturing, vol. 39, p. 1037-1053, 2008

[5] Harrison, P., Clifford, M.J., Long, A.C.: “Shear characterization of woven textile composites”, 10th European Conference of Composite Materials, Brugge, Belgium, 2002